Electronic band structures of group-V two-dimensional materials

Electronic Band Structures of Group-V Two-Dimensional Materials

Nuning Anugrah Putri Namari*, and Mineo Saito

Division of Mathematical and Physical Science, Graduate School of Natural Science and Technology, Kanazawa University, Kakuma-machi, Kanazawa 920-1192, Japan

We systematically study the electronic properties of 2D group-V materials, i.e phosphorene, arsenene, antimonene, and bismuthene. The density functional calculations are performed by using generalized gradient approximation. We first clarify that the α structure is the most stable in the cases of phosphorene and bismuthene and the β structure is the most stable in the cases of arsenene and antimonene. We next analyze the band structures based on the group theory. As a result, we find that all the bands are doubly degenerated at the boundaries of the first Brillouin zone in the α structures and the degeneracies are due to the symmetry of the materials. The band gaps of the β structures are found to be larger than those of the α structures. This tendency in the band gaps is explained based on the fact that the band gap increases as the sp hybridization becomes large. We find that buckling occurs in the α structures of antimonene and bismuthene due to the electron transfer from the higher atom to the lower atom.

1. Introduction

Two dimensional materials have been attracting scientific interests because of their novel electronic properties. Since the discovery of graphene in 2004[1,2] , group IV materials including silicene,[3–5] germanene[6] and stanene[7] have been extensively studied. In particular, the Dirac cone in the electronic band structures characterizes the electronic properties of these materials. In addition to the group IV materials, group V materials recently attracted scientific interests since phosphorene was successfully synthesized from black phosphorus in 2014.[8] Whereas electronic properties of group IV materials are characterized by the Dirac cone, group V materials are semiconductors with band gaps. It was found that phosphorene has a moderate band gap and is suitable for field-effect transistor material.[9,10] As well as the phosphorene, other group V materials, arsenene,[19–22,24] antimonene[23–26] and bismuthene[27–30] have recently studied.

The purpose of this paper is to systematically study the electronic structures of group V materials. We perform first-principles density-functional based calculations. The group

*E-mail: nuningapn@gmail.com

V materials form two types of structures, i.e., the α and β structures. We first clarify which structure is the most stable. Next we analyze the band structures based on the group theory. We also discuss the chemical trend for the band gap values.

2. Method

First, we explain how to idetify the irreducible representation of each band based on the group theory. We consider the electronic wave function $\Psi_i^{\boldsymbol{k}}(\boldsymbol{r})$ in a 2D periodic system, where i is the band index and k refers to the wavevector. The symmetry operation $\hat{R}$ is given by

$$\hat{R} = \{\Theta|\boldsymbol{\tau}\},$$

where Θ and $\boldsymbol{\tau}$ represent rotation and translation, respectively. When $\hat{R}$ operates the Bloch wavefunction $\Psi_i^{\boldsymbol{k}}(\boldsymbol{r})$, we obtain the following expression

$$\hat{R}\psi_i^{\boldsymbol{k}}(\boldsymbol{r}) = \psi_i^{\boldsymbol{k}}(\Theta^{-1}\boldsymbol{r} - \Theta^{-1}\boldsymbol{\tau}).$$

The projection operator $\hat{P}_{\boldsymbol{k}}^l$ is defined by

$$\hat{P}_{\boldsymbol{k}}^l = \frac{1}{h}\sum_R \chi_{\boldsymbol{k}}^l(\hat{R})\hat{R}, \tag{1}$$

where h is the order of the $\boldsymbol{k}$ group and l is the index of the irreducible representation, and $\chi_{\boldsymbol{k}}^l(\hat{R})$ is the character of the irreducible representation. To determine the irreducible representations of the wavefunctions $\psi_i^{\boldsymbol{k}}(\boldsymbol{r})$ which have the n-th degeneracy (i runs from j to $j+n$), we evaluate the following expression;

$$Q = \sum_{i=j}^{j+n}\int dr\psi_i^{\boldsymbol{k}}(\boldsymbol{r})^*\hat{P}_{\boldsymbol{k}}^l\psi_i^{\boldsymbol{k}}(\boldsymbol{r}). \tag{2}$$

When Q=1 (Q=0), the wavefunctions belong to (do not belong to) the l-th irreducible representation. We implemented the above mentioned method in the code PHASE/0,[32] so we can identify the representations by using computers. We hereafter use the irreducible ray representation:

$$\acute{\chi}_{\boldsymbol{k}}^l = \exp(i\boldsymbol{k}\cdot\boldsymbol{\tau})\chi_{\boldsymbol{k}}^l \tag{3}$$

Characters of the irreducible ray representation frequently correspond to those of Mulliken symbols[31], which are used in the analysis of molecules but there are some exceptions as mentioned in the next section. Hereafter, we use the ray irreducible representation and simply refer to it as a "irreducible representation".

We perform first-principles calculations based on the density functional theory

(DFT) by using PHASE/0.[32] The generalized gradient approximation (GGA) is used. A norm-conserving pseudopotential is used for the P atom and ultrasoft pseudopotentials are used for As, Sb and Bi atoms. For the calculation of two dimensional materials, we introduce the vacuum space around 20 Å in the z direction to avoid the interaction between neighboring slabs. As for the k-point sampling, we use the $15 \times 15 \times 1$ k-mesh. The spin orbit interaction gives some substantial effect on electronic properties of heavy atoms such as bismuth but since our purpose is to clarify the chemical trend of materials, we neglect the effect throughout the present study.

3. Results and Discussion

3.1 Optimized Structures and Stability

There are two types of α structures, i.e. non-buckled and buckled structures (Fig. 1). In the non-buckled structure, the two top atoms are equivalent and the space group is high, $Pmna(D_{2h}^7)$ whereas the buckled structure has the lower symmetry of $Pmn2_1(C_{2V}^7)$. We find that phosphorene and arsenene have the higher symmetry while antimonene and bismuthene have the lower symmetry. Optimized structural parameters are tabulated in Table.I. The bond angle θ_1 tends to be close to 90° as the atom becomes heavy. This is due to the fact that as the atom becomes heavy, the s orbital is relatively shrunk compared with the p orbital, thus sp hybridization becomes weak and bond angle becomes close to that of p^3 (90°).[11,12]

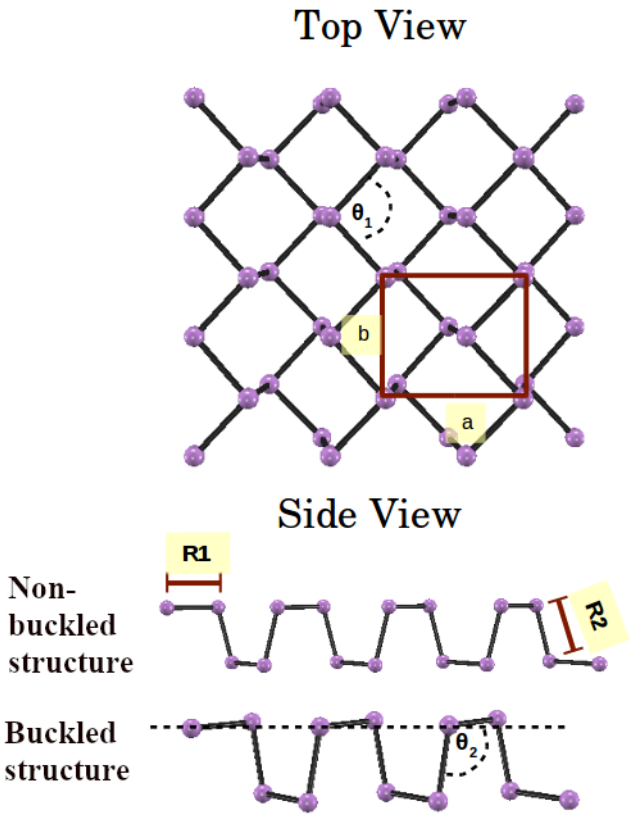

Fig. 1. Atomic structure of the α structure.

Table I. Calculated structural parameters of the α structures. Results calculated from GGA calculations in the past are also presented.

	a(Å)	b(Å)	R1(Å)	R2(Å)	θ_1(°)	θ_2(°)
P	4.52	3.37	2.25	2.28	96.82	102.78
GGA[17]	4.55	3.31	2.22	2.26	96	104
As	4.76	3.68	2.50	2.48	94.78	100.79
GGA[19]	4.76	3.67	2.50	2.48	94.64	100.80
Sb	4.73	4.29	2.91	2.84	94.63	103.95
GGA[23]	4.74	4.28	2.91	2.84	95.0	103.0
Bi	4.88	4.41	3.07	3.00	91.18	105.09
GGA[27]	4.87	4.44	3.08	3.03	92.2	106.7

The β structures are shown in Fig. 2. In the case of group-IV two-dimensional materials, graphene has the planar structure belonging to the space group of $P6/mcc(D_{6h}^2)$

whereas other systems such as silicene and stanene have buckled structures belonging to the space group of $P\bar{3}m1(D^3_{3d})$.[13] On the other hand, in the group V two-dimensional materials, all structures are buckled. Buckling height of group-V materials tends to be higher than group-IV materials;[35] the buckling height in the group-V materials are tabulated in Table II. As in the case of the α structure, the bond angle tends to become small and the amplitude of buckling increases as the atom becomes heavy (Table II). This is due to the fact that as the atom becomes heavy, s orbital is more localized, then the bond angle becomes close to the p^3 bond angle (90°) . As is seen in Tables I and II, the determined geometries of α and β structures are close to those obtained from GGA calculations in the past.

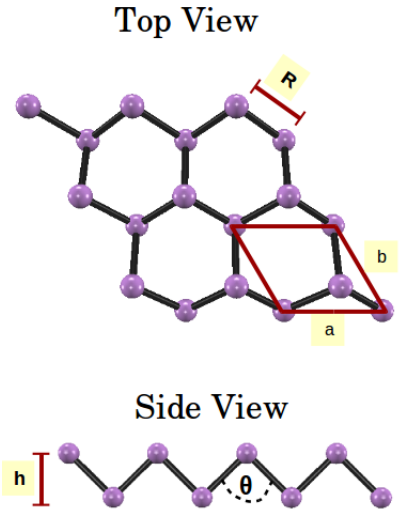

Fig. 2. Atomic structure of the β structure.

Table II. Calculated structural parameter of the β structures. Results calculated from GGA calculations in the past are also presented.

	a(Å)	R(Å)	θ(°)	h(Å)
P	3.27	2.25	92.55	1.24
GGA[18]	3.28	2.27	92.9	1.24
As	3.60	2.50	92.00	1.40
GGA[20]	3.61	2.51	91.95	1.40
Sb	4.08	2.86	90.77	1.63
GGA[20]	4.12	2.89	90.84	1.65
Bi	4.26	3.0	90.45	1.72
GGA[28]	4.39	3.07	91.24	1.73

We here calculate the cohesive energies of the α and β structures to find which structure is more stable for each material, where the cohesive energy is given by

$$E_c = (nE_{atom} - E_{material})/n.$$

In this expression, E_{atom} and n refers to total energy and the number of isolated atom, respectively, and $E_{material}$ is the calculated total energy of tow dimensional materials.

Table III. Calculated cohesive energy.

	E_c(eV/atom)	
	α structure	β structure
P	3.16	3.14
As	2.85	2.89
Sb	2.56	2.57
Bi	2.42	2.41

As is shown in Table III, we find that the α structures have higher cohesive energies in the cases of phosphorene and bismuthene and vice versa in the cases of arsenene and antimonene.[34)]

3.2 Electronic structures analyzed based on the group theory

By using the group theory, we identify the irreducible representations of bands in the α-structures (Fig. 3) and β-structures (Fig.4) . The special points used in both structures are shown in Fig.5. The k groups for special points and lines of the α structure are tabulated in Table IV. Since phosphorene and arsenene form non-buckled structures, their symmetries are higher than those of antimonene and bismuthene that form buckled structures. We used Mulliken symbols to denote the irreducible representations in the most parts of bands.[31)] However, some irreducible representations cannot be represented by Mulliken symbols. In the cases of phosphorene and arsenene (Fig. 3 (a) and (b)), the irreducible representations on the X-D-S-C-Y line cannot be denoted by Mulliken symbols and all of the bands on this line are doubly degenerated (Table.V). These doubly degenerated bands arise from the fact that the present system belongs to the non-symmorphic space group (D^7_{2h}).[33)]

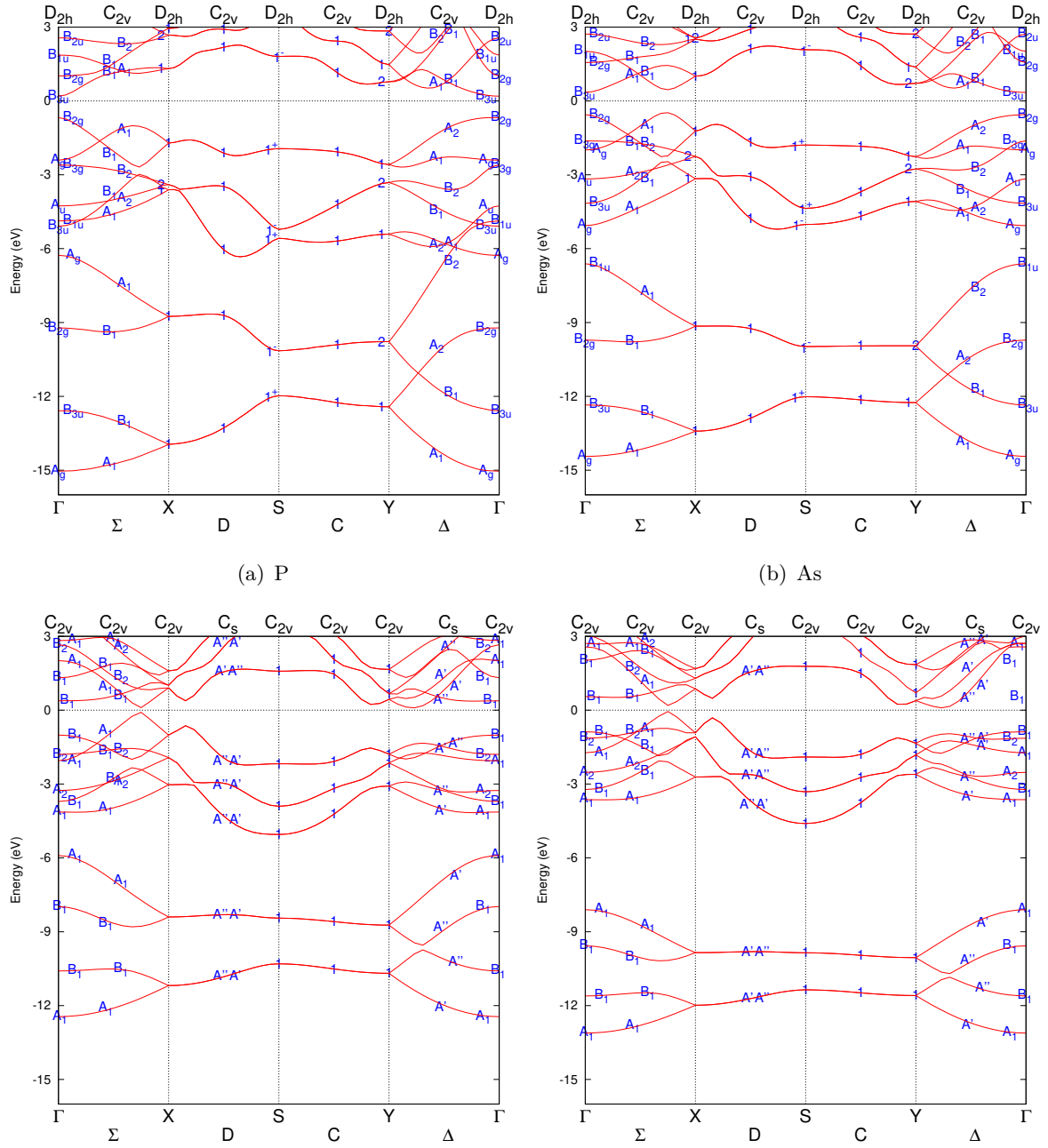

(a) P (b) As

(c) Sb (d) Bi

Fig. 3. Band structures of α-phosphorene (a), α-arsenene (b), α-antimonene (c), and α-bismuthene (d). When the irreducible representations cannot be denoted by Mulliken symbols, we use numerical notations (1,2,1^+ and 2^-) and the character table for these irreducible representations are given in Tables V and VI. In the other cases, we use Mulliken symbols (A_1,A_2,B_1, B_2 and so on).[31)]

Table IV. Space group and point group of each k-point in the α structure.

	Phosphorene & Arsenene	Antimonene & Bismuthene
Space Group	$Pmna(53, D_{2h}^7)$	$Pmn2_1(31, C_{2V}^7)$
Γ	D_{2h}	C_{2V}
Σ	C_{2V}	C_{2V}
X	D_{2h}	C_{2V}
D	C_{2V}	C_S
S	D_{2h}	C_{2V}
C	C_{2V}	C_{2V}
Y	D_{2h}	C_{2V}
Δ	C_{2V}	C_S

Table V. Character table of special points in α-phosphorene and α-arsenene.

		E	$C_2(x)$	$C_2(y)$	$C_2(z)$	I	σ_{yz}	σ_{xz}	σ_{xy}
$X(D_{2h})$	1	2	0	0	0	0	0	2	0
	2	2	0	0	0	0	0	-2	0
$D(C_{2V})$	1	2		0			0		0
$S(D_{2h})$	1^+	2	0	0	0	2	0	0	0
	1^-	2	0	0	0	-2	0	0	0
$C(C_{2V})$	1	2		0			0		0
$Y(D_{2h})$	1	2	0	2	0	0	0	0	0
	2	2	0	-2	0	0	0	0	0

We next study antimonene and bismuthene whose symmetries (C_{2V}^7) are lower than those of phosphorene and arsenene (Table IV). The irreducible representations on the S-C-Y lines cannot be denoted by using Mulliken symbols (Figs. 3 (c) and (d)) and all of the bands on those lines are doubly degenerated (Table VI) as in the cases of phosphorene and arsenene. However, unlike phosphorene and arsenene, the irreducible representations on the X-D line in antimonene and bismuthene can be denoted by Mulliken symbols (see Table VI). Although all the irreducible representations are one dimensional, the bands are doubly degenerated. This accidental degeneracy is due to

the pairing of two bands belonging to different representations, which is caused by the time-reversal symmetry.[33] We conclude that in both cases of non-buckled and buckled structures, the bands are doubly degenerated on the X-D-S-C-Y line. These peculiar band structures are expected to be detected by using some experiments such as photoelectron spectroscopy.

Table VI. Character table of special points in α-antimonene and α-bismuthene.

		E	$C_2(x)$	σ_{xz}	σ_{xy}	σ_h
$X(C_{2v})$	$1(A_1)$	1	1	1	1	
	$2(A_2)$	1	1	−1	−1	
	$3(B_1)$	1	−1	1	−1	
	$4(B_2)$	1	−1	−1	1	
$S(C_{2v})$	1	2	0	0	0	
$C(C_{2v})$	1	2	0	0	0	
$Y(C_{2v})$	1	2	0	0	0	
$D(C_S)$	$1(A')$	1				1
	$2(A")$	1				−1

As Fig. 4 shows, unlike the α-structures, boundaries of the first Brillouin zone in β-structures can be denoted by Mulliken symbols. There are no doubly degenerated bands at the boundaries of the first Brillouin zone. The difference between the α and β structures originates from the fact that β-structures ($P\bar{3}m1$) are symmorphic system. β structures have the same symmetry as those of silicene. However, unlike the group IV materials,[13] the Dirac cone does not appear at the Fermi level in the case of the β-structure.

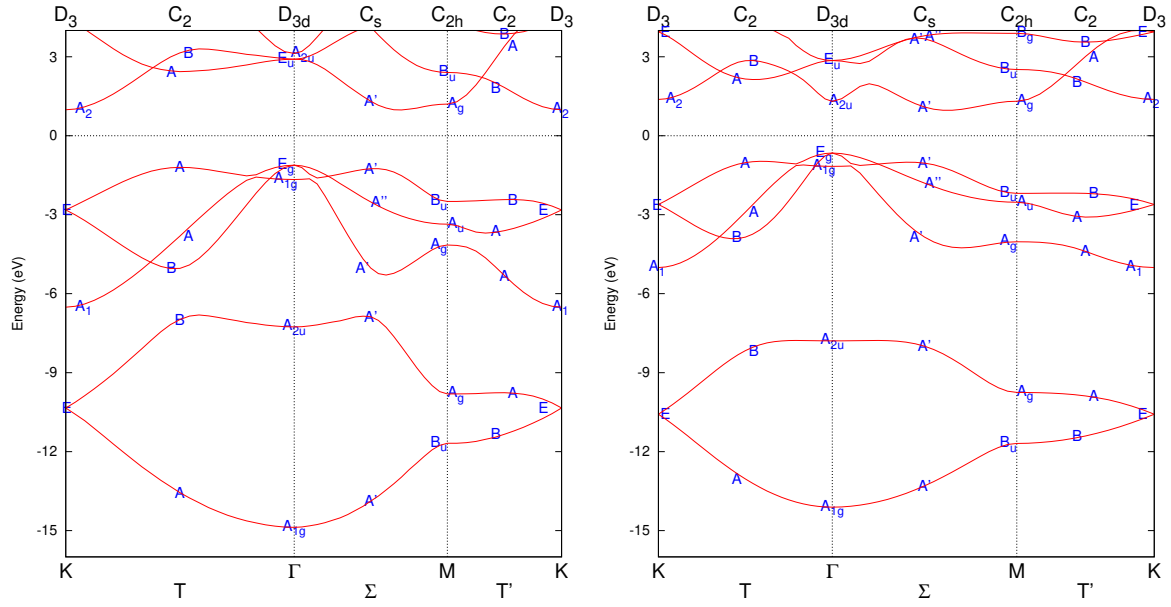

(a) P (b) As

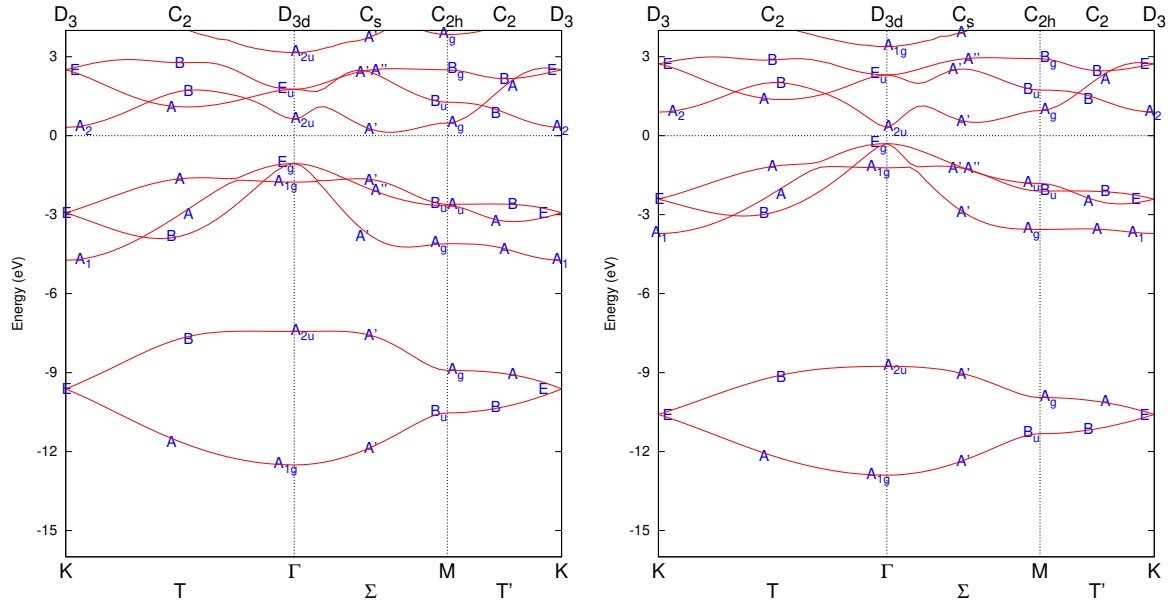

(c) Sb (d) Bi

Fig. 4. Band structures of β-phosphorene (a), β-arsenene (b), β-antimonene (c), and β-bismuthene (d). We use Mulliken symbols for one dimensional irreducible representations (A_1,A_2,B_1, B_2 and so on) and for two dimensional ones (E, E_g and E_u)[31)]

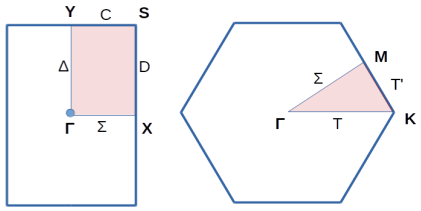

(a) (b)

Fig. 5. Brillouin zone of the α structure (a) and β structure (b).

3.3 Energy band gap

Figure 3 shows the electronic band structures of the α structures. All the α structure materials have direct band gaps. On the contrary, all of the β structure materials have indirect band gaps except for bismuthene as shown in Fig.4, but if we include SOC in the calculation, bismuthene also has an indirect band gap as reported in a previous paper.[27] We find that the band gaps of the β-structures are larger than those of the α-structures (Table.VII).

Table VII. Energy band gap.

	α structure (eV)	β structure(eV)
P	0.83	2.10
As	0.80	1.57
Sb	0.33	1.16
Bi	0.26	0.60

We here calculate the partial density of states (PDOS) (Fig.6). In both α and β structures, the lowest bands have s character as shown in Fig.6. This s band width decreases as the atom becomes heavy, which is due to the fact that the s orbitals become relatively localized compared with p orbitals and thus the overlap between the neighboring s orbitals becomes small. Therefore the sp hybridization becomes weak as the atom becomes heavy, which is the reason why the bond angles tend to become close to p^3 bond angle (90°) as the atom becomes heavy. However, it is noted that both valence and conduction bands near the Fermi level include s and all p components and thus the present systems have weak sp hybridization. The insets in Fig.6 show the s-orbital contribution around the Fermi level and we find that β-structures have higher contributions of s-orbitals than those of α-structures. Therefore, the sp-hybridization in

β-structures is stronger than α-structures. This sp hybridization is expected to enlarge the band gaps as discussed below.

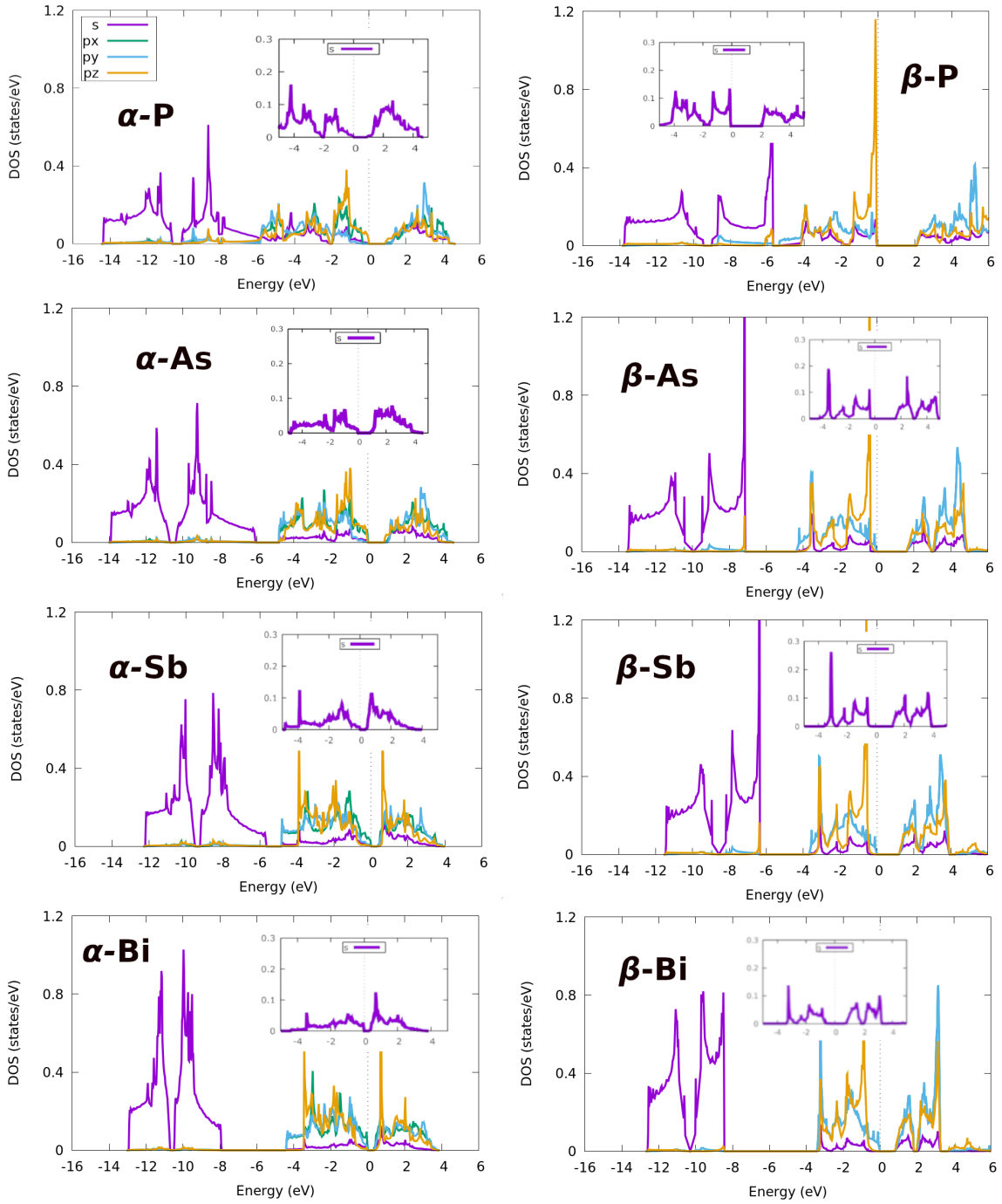

(a) (b)

Fig. 6. PDOS of α-structure(a) and β-structure(b).

Figure 7 shows the density of states (DOS) and partial charge density at the Fermi level in the α and β structures of arsenene. The charge density of α-structure shows p bonding (anti-bonding) character for the valence band top (conduction band bottom) as is seen in Fig. 7(a). Since the p bond is weak, the band gap of the α structure is small. On the contrary, the sp hybridization in the β-structure is relatively strong. Since sp-hybridized bonding is strong, the band gap in the β structure is large.

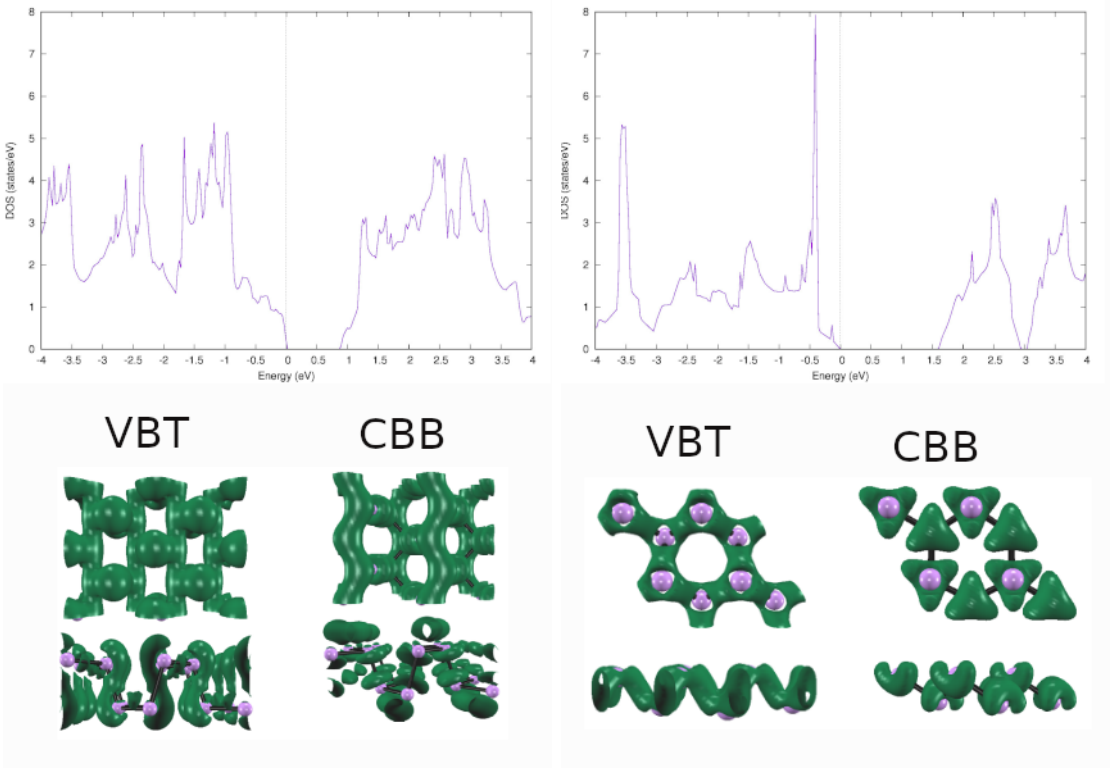

(a) (b)

Fig. 7. DOS and charge density on valence band top (VBT) and conduction band bottom (CBB) of α-arsenene (a) and β-arsenene (b).

We next study antimonene (Fig.8). We find that the α structure shows p bonding and p anti-bonding characters in highest valence and lowest conduction band, respectively (fig.8(a)). Since pure p bond is weak, the energy band gap is small. On the contrary, β-structure shows the sp-bonding character for the valence and top and sp-anti-bonding character for the conduction band bottom just like those in arsenene (fig.8(b)). These differences in characters between the α and β structures are the reason why the β structure has a larger band-gap than α-structure. As discussed above, we find that in the cases of arsenene and antimonene,the sp hybridization is relatively strong in the

β structures,which induces large band gaps of the β structures. In phosphorene and bismuthene, we also find that sp hybridization is relatively large in the β structure and the relatively large band gaps are induced in the β structures.

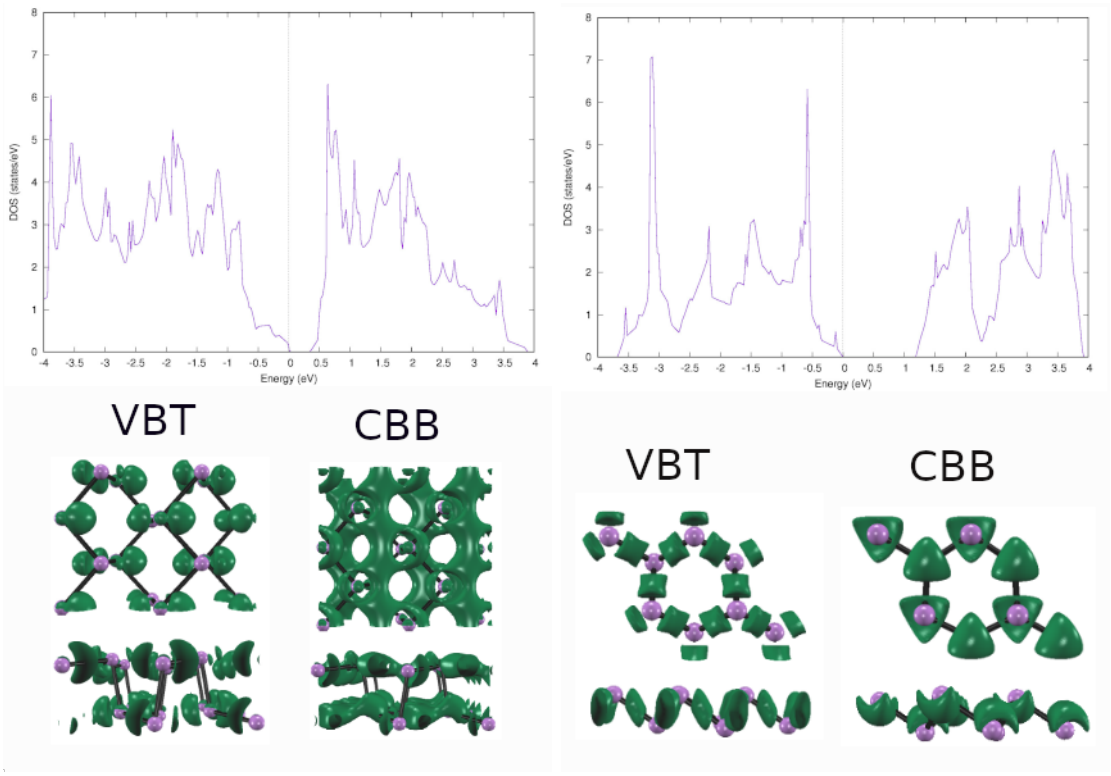

(a) (b)

Fig. 8. DOS and charge density on valence band top (VBT) and conduction band bottom (CBB) in α-antimonene (a) and β-antimonene (b).

3.4 Buckling mechanism

As reported in a previous section, in the α structures, phosphorene and arsenene are not buckled and antimonene and bismuthene are buckled. The buckling mechanism of bismuthene has been already clarified in a previous paper.[12] We here discuss the mechanism of buckling in antimonene, which is similar to that in bismuthene.

We first compare the band structures of the non-buckled and buckled structures of antimonene (Fig.9). We find that the energy difference between the highest occupied and lowest unoccupied levels at the Γ point becomes large when the buckling occurs. This enlargement of the energy difference is expected to be due to the electron-lattice interaction;[12] since the buckling motion belongs to the Γ point, the energy difference at the Γ point becomes large. In the non-buckled structure, the two top atoms are

equivalent and they become inequivalent due to the buckling. In the buckled structure, the amplitude of the wavefunction of the higher (lower) atom is small (large) in the highest occupied state and vice versa in the lowest unoccupied state (Fig. 9). This fact means that the orbital of the lower atom has the lower energy than that of the higher atom. The electron transfer increases the population of the lower energy orbital, which leads to the fact that the buckled structure has a lower total energy than the non-buckled structure.

We conclude that the buckling is induced in antimonene because of the fact that the two top atoms become inequivalent and the electron transfers from the higher atom to the lower atom due to electron-lattice interaction. This electron transfer was also found in bismuthene.[12)] We find that phosphorene and arsenene are not buckled. This is expected to originate from the fact that these materials have large band gaps in the non-buckled structures and thus the buckling does not stabilize the systems.

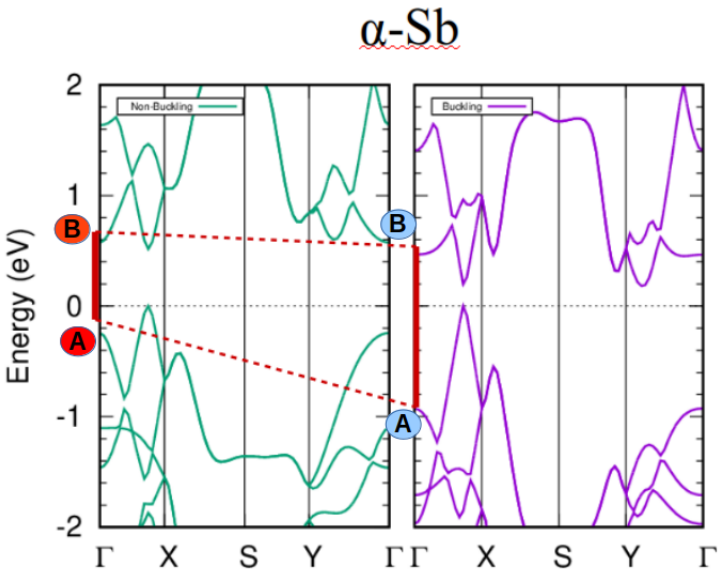

(a)

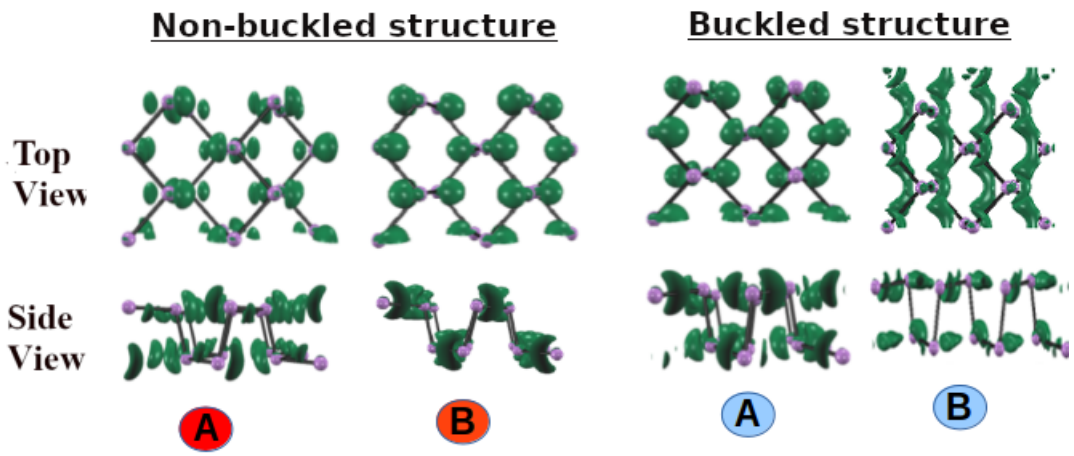

(b)

Fig. 9. Band structures of α-Sb (a) non-buckling (green line) and buckling (purple line) with charge distribution in non-buckling (b)

4. Conclusions

We performed DFT calculations of group-V 2D materials, i.e., phosphorene, arsenene, antimonene and bismuthene. We first clarify that the α structure is the most stable in the cases of phosphorene and bismuthene and β structure is the most stable in the cases of arsenene and antimonene. We next analyze the band structures based on the group theory. As a result, we find that all the bands are doubly degenerated at the boundaries of the first Brillouin zone in the α structures, and the degeneracies are due

to the symmetry of the materials. On the contrary, these degeneracy does not appear in the case of β structures. The band gaps of the β structures are found to be larger than those of the α structures. This tendency in the band gaps is explained based on the fact that the band gap increases as the sp hybridization becomes large. We find that buckling occurs in the α structures of antimonene and bismuthene due to the electron transfer from the top atom to the lower atom.

5. Acknowledgement

This work was partly supported by Grants-in-Aid for Scientific Research (No. 17K05118) from the Japan Society for the Promotion of Science (JSPS). The computations in this research were performed using the supercomputers at the Institute for Solid State Physics (ISSP)at the University of Tokyo.

References

1) K.S.Novoselov, A.K. Geim, S.V.Morozov, D.Jiang, Y.Zhang, S.V. Dubonos, I.V. Grigorieva, and A.A. Firsov, SCIENCE.306,666(2004)
2) K.S.Novoselov, and A.K. Geim, nature materials.6,183(2007)
3) P. Vogt, P.D. Padova, S. Quaresima, J. Avila, E. Frantzeskakis, M.C. Asensio, A.Resta, B. Ealet, and G.L. Lay, Phys.Rev.Lett.108,155501(2012)
4) S. Huang, W. Kang, L. Yang, Appl.Phys.Lett.102,133106(2013)
5) K.Takeda, and K.Shiraishi,Phys.Rev.B.50,14916(1994)
6) E. Blanco, S. Butler, S.Jiang, O.D. Restrepo, W. Windi, and J.E. Goldberger ACS Nano.7,4414(2013)
7) F. Zhu, W Chen, Y. Xu, C. Gao, D. Guan, D.Qian, S.Zhang, and J. Jia, Nature Materials.14,1020(2015)
8) H.Liu, A.T. Neal, Z. Zhu, Z. Luo, X. Xu, D. Tomanek, and P.D. Ye, ACS Nano.8,4033(2014)
9) L.Liu, Y.Yu, G.J. Ye, Q. Ge, X. Ou, H. Wu, D. Feng, X.H. Chen, and Y. Zhang, Nat.Nanotechnol.9,372(2014)
10) T. Hong, B. Chamlagain, W. Lin, H.J. Chuang, M. Pan, Z. Zhou, and Y.Q. Xu, Nanoscale.6,8978(2014)
11) Z.Tang, M.Hasegawa, T.Chiba, M. Saito, H.Sumiya, Y.Kawazoe, and S.Yamaguchi,Phys.Rev.B.57,12219(1998)
12) M.Saito, Y.Takemori, T.Hashi, T.Nagao, and S.Yaginuma,Jpn.J.Appl.Phys.46,7824(2007)
13) S.Minami, I.Sugita, R.Tomita, H.Oshima, and M. Saito,Jpn.J.Appl.Phys.56,105102(2017)
14) R.Hultgren, N.S.Gingrich, and B.E.Warren,J.Chem.Phys.3,351(1935)
15) Y.Ding, and Y. Wang, J.Phys.Chem.C.119,10610(2015)
16) J.Guan, Z.Zhu, and D. Tomanek, Phys.Rev.Lett.113,046804(2014)
17) V.Vierimaam, A.V.Krasheninnikov,and H.P Komsa, Nanoscale.8,7949(2016)
18) M.Sun, S.Wang, J.Yu, and W. Tang,Appl.Surf.Sci.392,46(2017)
19) C.Kamal, and M. Ezawa, Phys.Rev.B.91,085423(2015)
20) Y. Xu, B.Peng, H.Zhang, H.Shao, R. Zhang, and H. Zhu,Ann.Phys.(Berlin).529,1600152(2017)
21) M.Pumera, and Z. Sofer, Adv.Mater.29,1605299(2017)

22) G. Moynihan, S. Sanvito, and D. D O'Regan,2D Mater.4,045018(2017)
23) O.U.Akturk, V.O.Ozcelik, and S. Ciraci, Phys.Rev.B.91,235446(2015)
24) S.Sharma, S.Kumar, and U. Schwingenschlögl, Phys.Rev. Appl.8,044013(2017)
25) M.F.Deschênes, O.Waller, T.O. Menteş, A.Locatelli, S. Mukherjee, F. Genuzio, P. L. Levesque, A. Hébert, R. Martel, and O. Moutanabbir, Nano Lett.17,4970(2017)
26) P. Ares, J. J. Palacios, G. Abellán, J. G. Herrero, and F. Zamora, Adv. Mater.1703771(2017)
27) E. Akturk, O.U. Akturk, and S.Ciraci, Phys.Rev.B.94,014115(2016)
28) M.Y.Liu, Y.Huang, Q.Y.Chen, Z.Y.Li, C.Cao, and Y.He, RSC Adv.7,39546(2017)
29) T. Nagao, J.T. Sadowski, M. Saito, S. Yaginuma, Y. Fujikawa, T. Kogure, T. Ohno, Y. Hasegawa, S. Hasegawa, and T. Sakurai, Phys. Rev. Lett.93.105501(2004)
30) M. Saito, T. Ohno, T. Miyazaki, Appl. Surf. Sci.237.80(2004)
31) R. S. Mulliken, J. Chem. Phys.23. 1997(1955);24. 1118 (1956)
32) PHASE/0 [https://azuma.nims.go.jp/]
33) G.Burns,Introduction to Group Theory with Applications,ed.A.M.Alper, and A.S.Nowick(Academic Press,New York,1977)p.323.
34) S.Zhang, S.Guo, Z.Chen, Y.Wang, H.Gao, J.G.Herrero, P.Ares, F.Zamora, Z.Zhu, and H.Zeng, Chem.Soc.Rev.47.982(2018)
35) B.Mortazavi, O.Rahaman, M.Makaremi, A.Dianat, G.Cuniberti, and T.Rabczuk, Physica E.87.228(2017)